

1 Supplemental Information

2

3 ACSS2 gene variants determine kidney disease risk by controlling
4 de novo lipogenesis in kidney tubules

5 Dhanunjay Mukhi^{1,2,3}, Lingzhi Li^{1,2,3}, Hongbo Liu^{1,2,3}, Tomohito Doke^{1,2,3}, Lakshmi P. Kolligundla,
6 Eunji Ha^{1,2,3}, Konstantin Kloetzer^{1,2,3}, Amin Abedini^{1,2,3}, Poonam Dhillon^{1,2,3}, Sarmistha
7 Mukherjee^{2,4}, Junnan Wu^{1,2,3}, Hailong Hu^{1,2,3}, Dongyin Guan⁵, Katsuhiko Funai⁶, Kahealani
8 Uehara^{2,4}, Paul M. Titchenell^{2,4}, Joseph A. Baur^{2,4}, Kathryn E. Wellen^{7,8}, Katalin Susztak^{1,2,3,9*}

9

10

11 **Inventory for Supplemental Information**

- 12 I. Supplemental methods
- 13
- 14 II. References
- 15
- 16 III. Supplemental Figure 1. Prioritization of ACSS2 as a kidney disease risk gene.
- 17
- 18 IV. Supplemental Figure 2. Loss of ACSS2 protects from kidney disease.
- 19
- 20 V. Supplemental Figure 3. TGF- β 1 induces de novo lipogenesis in primary tubule cells.
- 21
- 22 VI. Supplemental Figure 4. Inhibition of de novo lipogenesis prevents kidney fibrosis.
- 23
- 24 VII. Supplemental Figure 5. Suppression of mitochondrial ROS suppresses NLRP3-
25 inflammasome activation in primary tubular cells.
- 26
- 27 VIII. Supplemental Figure 6. Inhibition of de novo lipogenesis suppresses ROS-induced
28 NLRP3 inflammasome activation.
- 29
- 30 IX. Supplemental Figure 7. Fatty acid synthesis correlated with fibrosis in CKD patients.
- 31
- 32 X. Supplementary Table 1: Gene prioritization table.
- 33
- 34 XI. Supplementary Table 2: Prioritized SNPs.

35 XII. Supplementary Table 3. Guide RNAs and human primers.

36

37 XIII. Supplementary Table 4: Mouse gene primers.

38

39 **Supplemental methods**

40

41 **Prioritization of causal genes for eGFR GWAS loci**

42 To prioritize target genes for eGFR GWAS loci on chr 20, we employed a priority scoring strategy
43 by integrating eight different datasets: (1) microdissected kidney tubule and glomeruli eQTL data
44 sets (https://susztaklab.com/Kidney_eQTL/index.php) (significant SNP~gene associations,
45 FDR<0.05)(1, 2); (2) mQTL (significant SNP~CpG~gene associations, FDR<0.05) and eQTM
46 (CpG level FDR <0.05) analysis (https://susztaklab.com/Kidney_meQTL/index.php) (3); (3)
47 colocalization between eGFR GWAS and eQTL ($H4 > 0.8$); (4) multiple colocalization (moloc)
48 analysis(3) of SNP~gene pairs between eGFRGWAS, eQTL and mQTL (PPA.abc > 0.8); (5)
49 summary mendelian randomization for the SNP~gene pairs between eGFR GWAS and eQTL
50 (PSMR < 1.38×10^{-4}); (6) SNP~gene pairs passing HEIDI test between eGFR GWAS and eQTL
51 (PHEIDI > 0.01); (7) Cicero co-accessibility interactions data from 57,262 snATAC-seq cells (co-
52 accessibility score > 0.2)(https://susztaklab.com/Human_snATAC/index.php) (2, 3); and (8)
53 Element-gene connections identified by Activity-by-Contact (ABC) model which predicts
54 enhancers regulating genes based on estimating enhancer activity and enhancer-promoter
55 contact frequency from epigenomic datasets (ABC scores ≥ 0.015)(4). Promoters were defined
56 as ± 2000 bp from the TSS of protein-coding transcripts from GENCODE v35lift3765 to annotate
57 Cicero connections or Element-gene connections between gene promoters and eGFR GWAS
58 variants. eGFRcrea GWAS meta-analysis, (n=1,508,659 individuals), DNA methylation data
59 (n=506 human kidneys), cis-eQTL, kidney mQTL (n=686 individuals) and Bayesian colocalization,

60 and summary Mendelian randomization analyses were performed according to previous
61 publication (2, 3).

62

63 **Human kidney single nuclear ATAC-sequencing**

64 Adult human kidney single nuclear ATAC seq- data was used from previous publications (2, 3).

65 The data can be viewed at the website (http://www.susztaklab.com/Human_snATAC/index.php).

66 **Animal studies**

67 The mice were fed *ad libitum* with water and rodent standard chow diet. 6- to 7-week-old male
68 and female C57BL/6J mice were used in the study. Mice were randomly assigned to experimental
69 groups for all experiments including drug efficacy studies. To induce kidney injury, we employed
70 two widely used kidney disease models including unilateral ureteral obstruction (UUO) and folic
71 acid nephropathy (FAN). UUO surgery experiments were conducted on male and female mice.
72 Briefly, UUO was performed by ligating the right kidney ureter, and the left kidney served as a
73 sham operated kidney. Post-surgical procedures were followed according to the IACUC
74 guidelines. For FAN models, 300mM sodium bicarbonate (NaHCO₃) solution was first made to
75 solubilize folic acid (FA) and injected into male mice (FA 250 mg/kg i.p at single dose). Mice were
76 sacrificed 7 days following injection or surgery. For the drug injection studies, mice were first
77 injected one day before the UUO surgery.

78

79 **Adenine induced chronic kidney disease model**

80 Adenine (#A11500) was purchased from RPI (Saint Louis, MO, USA). Adenine was dissolved in
81 water at a concentration 2.5 mg/ml. Male mice were given adenine by oral gavage at a dose of
82 50mg/kg body weight daily for four weeks (5). Control male mice received 0.2ml of vehicle every
83 day for four weeks. Animals were sacrificed on day 30. BUN and serum creatinine was analyzed

84 by BUN (#B7552-150, Horiba Pointe Scientific) and creatinine kits (#DZ072B-KY1, Diazyme).
85 Daily body weights were recorded.

86

87 **Crispr SNP deletion experiments**

88 Two Crispr guides were generated for the open chromatin of the prioritized SNP region. Guide
89 RNAs were designed using Crispor software(6) and cloned into pLKO5.SgRNA.EFS.GFP plasmid
90 (#57822, Addgene) using Esp3I restriction enzyme (#FD0454, Thermo). Guide RNA sequences
91 and human primers were listed in Supplemental table 3. Bacterial transformation was performed
92 using OneShot-Stbl3 competent cells (#C737303, Thermo) and isolated plasmids were verified
93 by Sanger sequencing. The guide RNA containing plasmids were transfected into HEK293 cells
94 stably expressing Cas9 (gift from Dr. Liling Wan, University of Pennsylvania) using Lipofectamine
95 3000 (#L300015, Thermo). After 72h of transfection, puromycin (4µg/ml) was added for an
96 additional 3 days. The cells were harvested, and RNA, and DNA were isolated. The DNA was
97 cloned into TOPO-TA vector and TOP10 chemical competent cells (#K4500J10, Thermo).
98 Genomic region deletion was further verified by Sanger sequencing. The isolated RNA was used
99 to measure gene expression by quantitative real time PCR.

100

101 **Gene expression analysis**

102 A total of 15mg of kidney tissue was homogenized in 1ml of Trizol (Ambion) with Qia Tissue Lyzer
103 for 1min 15sec at 4°C. After homogenization in Trizol, 200ul of chloroform was directly dispensed
104 into the Trizol lysate and vortexed for 15sec at RT. Lysates were then spun down at 12000rpm
105 for 15min at 4°C, and the upper aqueous layer was collected into new, clean tubes. Next, 500ul
106 of isopropanol (100%) was slowly added through the wall of the tubes and mixed gently. The
107 tubes were then spun down at 12500rpm at 4°C for 15min, and the pellet was washed with 70%

108 ethanol (made from clean 100% ethanol) at 10000rpm for 10min at 4°C. Finally, the RNA pellet
109 was dried at RT for 15min, resuspended in clean RNase free and Dnase free water. RNA was
110 pretreated with DNase before proceeding to cDNA conversion. A total of 2,000 ng RNA was
111 converted into cDNA using the High-capacity cDNA Reverse Transcription Kit (#4368813, Applied
112 Biosystems). Realtime quantitative PCR analysis was performed to measure the relative gene
113 expression by normalizing the CT values of gene of interest with endogenous control gene
114 (*Gapdh* was used). The data was calculated and presented as fold change by ($2^{-\Delta\Delta CT}$ method).
115 Primer sequence listed in Supplemental table 4.

116

117 **Western blotting**

118 Approximately 20-30mg of kidney tissue was homogenized in SDS-blue loading buffer (#7722,
119 CST) containing 42mM DTT. Samples were loaded onto the SDS-PAGE gels and run at 100v for
120 1h 40min at RT in Tris-Glycine-SDS buffer. The proteins were transferred onto a PVDF
121 membrane. Membranes were blocked with 3% non-fat dry milk powder in tris-buffer saline
122 containing Tween-20 (TBST) for 30min at RT. The blots were then incubated with primary
123 antibody overnight at 4°C. The primary antibodies used were anti-ACSS2 (#ab66038, abcam),
124 anti- α -SMA (#A5228, Sigma), anti-fibronectin (#ab2413, abcam), anti-NLRP3 (#AG-20B-
125 0014C100, Adipogen), anti-cleaved GSDMD (#36425S, CST), anti-human GSDMD (#sc-393656,
126 Santa Cruz), anti-CASPASE1 (#AG-20B-0042-C100, Adipogen), anti-FASN (#3180S, CST), anti-
127 PLIN2 (#PA5-29099, Invitrogen), anti-SCAP (#PA5-28982, Invitrogen), anti-KIM1 (#PA5-79345,
128 Invitrogen), anti-LC3 (#2775S, CST), anti-PARK2 (#sc-32282, Santa Cruz), and anti-GAPDH
129 (#2118S, CST). After primary antibody incubation, the blots were washed three times with TBST,
130 IRdye-conjugated secondary antibodies were probed for 1h at RT. The secondary antibodies
131 used were anti-rabbit IgG (H+L) (DyLight™ 800 4X PEG Conjugate, #5151S, CST) and anti-
132 mouse IgG (H+L) (DyLight™ 680 Conjugate, #5470S, CST). Finally, the blots were washed in

133 TBST for three minutes each, 10min at RT, and scanned at 600, 700, and 800 excitation
134 wavelengths in Li-COR imager (Odyssey® XF), Image Studio software. The images were
135 quantified for relative abundance in Image J software.

136

137 **Immunofluorescence staining**

138 Immunofluorescence performed as previously described(7). Briefly, 5µm thin formalin-fixed
139 paraffin-embedded kidney cortical sections were deparaffinized and rehydrated using ethanol
140 gradients from 100%-70%. Slides were preheated in a 10mM citrate buffer containing 0.1% triton
141 X-100 to retrieve the target antigen. The slides were blocked with PBS containing 10% BSA and
142 0.1% Tween for 1h at RT. The slides were incubated overnight at 4C with primary antibodies
143 prepared in PBS. The following primary antibodies were used: anti-Ki67 1:50 dilution (#9129S,
144 CST), anti-ACSS2 1:50 dilution (#ab66038, abcam), anti-FASN at 1:50 dilution (#3180S, CST),
145 and anti-Perilipin2 at 1:50 dilution (#PA5-29099, Invitrogen). LTL-Fluorescein (FL-1321, Vector
146 labs) was used to label PT cells. The slides were then incubated at 37OC with anti-rabbit Alexa
147 Fluor 488 (#A-21200, Invitrogen), and anti-mouse Alexa Fluor 594 (#A-31572, Invitrogen). Finally,
148 the sections were stained with DAPI containing anti-fade mounting media (#P36941, Invitrogen).

149

150 **Histone extraction and western blotting**

151 To extract histones from kidneys, we first isolated nuclei and proceeded with acid-histone
152 extraction method (8). Briefly, we washed nearly 40mg of kidney tissue with ice-cold PBS and
153 minced it in the nuclei isolation buffer (NIB-250 is 15mM Tris-HCl at pH 7.5, 60mM KCl, 15mM
154 NaCl, 5mM MgCl₂, 1mM CaCl₂, and 250mM sucrose, to which 0.1% Nonidet P-40, 1x protease
155 inhibitor cocktail, 1mM DTT, and 10mM sodium butyrate). We collected the kidney pieces into
156 glass Dounce homogenizer on ice. After 5 min of incubation on ice, we spun down the

157 homogenates, collected the nuclei pellet, washed it twice with NIB-250 without Nonidet P-40 and
158 proceeded with histone extraction.

159 We incubated the nuclear pellet with 0.4 N H₂SO₄ at a 5:1 ratio for 2h at 4°C. We then spun down
160 the acidified nuclei at 11000rcf for 10min at 4°C and collected the soluble fraction containing
161 histones into a new tube and precipitated with 20% trichloroacetic acid at final concentration
162 overnight at 4°C. We spun down the samples at 11000rcf for 10min at 4°C to sediment the histone
163 pellet at the bottom of the tube. We then washed the histone pellets with 1ml of ice-cold acetone
164 containing 0.1% 12N HCl, followed by two washes with ice-cold 100% acetone. We air-dried the
165 pellet and dissolved them in RIPA buffer. Two micrograms of histone lysates were loaded onto
166 15% SDS-PAGE gels. Western blotting was performed as described above and probed with anti-
167 H3K27ac (#ab177178, abcam) and anti-total H3 (#4620, CST) antibodies. Imaged in Li-COR
168 imager (Odyssey® XF).

169

170 **H&E and Sirius Red staining**

171 The tissues were fixed in formalin, dehydrated by an ethanol gradient (30%, 50%, 75% and 95%)
172 and then submitted to the histology Core in 100% ethanol. Once the tissue was sectioned, H&E
173 and Sirius red staining was performed. Images were acquired in Olympus 5000 microscope with
174 Cell Sense software. Percentage of relative fibrosis was quantified in image J.

175

176 **Primary tubular epithelial cell isolation and *in vitro* experiments**

177 Primary kidney tubular epithelial cells (TECs) were isolated from young pups (2.5-3wk old) of WT,
178 *Acss2*^{-/-}, *Fasnf*^{-/-} and *Scapf*^{/f} mice. Kidneys were collected on a petri dish on ice, minced in RPMI
179 media (Corning), and then then digested with 200ug/ml collagenase IV (1mg/ml, calbiochem) at

180 37°C for 30min. Collagenase was inactivated by adding 100µl of fetal bovine serum (100% FBS),
181 and cells were passed through 100µm, 70µm and finally 40µm strainers. Cells were then
182 centrifuged at 1000rpm for 5min at 4°C. The cell pellet was resuspended in 1 ml of sterile ice-
183 cold RBC lysis buffer (Hy-Clone) and incubated for 2min on ice. Lysis was inhibited by adding ice-
184 cold PBS and then centrifuged at 1000rpm for 10min at 4°C. Finally, the cell pellet was
185 resuspended in RPMI complete media (10% FBS with antibiotics 1X ITS and 50ng/ml human
186 EGF) and plated in 10cm dishes. Cells were grown in the incubator at 5% CO₂ at 37°C, and the
187 medium was changed every other day.

188 Cells were serum restricted in 0.5% FBS for 24h. Cells were then treated with 20ng/ml TGF-β1
189 for 48h in the presence or absence of FASNall (4µM/ml) or TVB-3664 (10nM/ml) in 0.5% serum
190 media for 48h. *Fasnf*^{-/-} or *Scap1*^{ff} cells were treated with adenovirus Ad5CMV-eGFP (Ad-GFP) or
191 Ad5CMVCre-eGFP (Ad-Cre-GFP) (University of Iowa Gene Transfer Vector Core, Iowa City, IA)
192 at a concentration of 0.5µl/ml for 24h in serum free media, and the infection efficiency was
193 assessed by observing GFP signal under a fluorescence microscope before every experiment.

194 For, *siRNA* transfection experiments, a smart pool of non-target control *siRNA* and mouse *siFasn*
195 were purchased from Dharmacon (#L-040091-00-0005, Horizon Biosciences). Cells were seeded
196 in 6-well plates, grown overnight at 80-90% confluent, and then transfected with 20pM *siFasn* in
197 RNAimax in OptiMEM for 48h. After transfection, cells were treated with TGF-β1 (20ng/ml) for
198 48h in 0.5% serum containing media. RNA or protein was isolated from these cells, and
199 knockdown efficiency was determined by quantifying the relative *Fasn* expression using real time
200 qPCR.

201 **Cholesterol measurement**

202 Total kidney cholesterol was quantitatively estimated using established methods (#K603-100,
203 BioVision). Approximately 10-15mg of kidney tissue was homogenized in 300 µl of chloroform:

204 isopropanol: NP-40 (7:11:0.1) in a microcentrifuge. The homogenate was centrifuged at 15000g
205 for 10min, and the liquid layer was collected into a new microtube. The supernatant was air dried
206 at 50°C to remove chloroform and the samples kept under vacuum pressure (SpeedVac, Thermo
207 Scientific) for 30 min to remove trace organic solvent. The dried lipids were dissolved in 200 µl of
208 assay buffer and performed cholesterol measurements as per the manufacturer protocol.

209

210 **³H labeled FAO measurements in mice kidneys**

211 FAO measurements were performed by tracing tritium labeled water (³H₂O) (9). Frozen whole
212 kidney extracts prepared in Krebs-Ringer bicarbonate buffer containing HEPES (#K4002, Sigma).
213 Nearly 500µg of protein was used for FAO measurements. Briefly, the kidney homogenates were
214 incubated with master cocktail (Krebs-Ringer bicarbonate buffer containing 100mg/ml fatty acid
215 free BSA, 2.5mM palmitic acid, 10mM carnitine, and 4µCi of 9,10-³H-palmitoyl-CoA) for 2h at
216 37OC and 600rpm in dark. The homogenates were then subjected to Folch's lipid extraction
217 protocol (2:1 chloroform and methanol) and further precipitated with 10% trichloro acetic acid
218 (#T6399, Sigma). After high-speed centrifugation at 4C, 1ml of supernatants were passed through
219 activated AG 1-X8 resin formate columns (#7316221, BioRad) and eluted in roughly 1ml volume
220 (³H₂O) into glass vials. Nearly 500ul of elutes were mixed into 3ml of scintillation cocktail and
221 read in a liquid scintillation counter (Beckman Coulter). The radioactive counts were subtracted
222 from the sample containing no protein and from sample with cold palmitic acid (#P5585, Sigma).
223 The final counts were normalized to the control samples and presented as relative FAO rate.

224

225 **In vitro palmitic acid oxidation test by Seahorse analyzer**

226 Real-time fatty acid oxidation analysis was performed in renal tubule cells using an XF-96
227 Extracellular Flux Analyzer with the Palmitate Oxidation Stress Test Kit and FAO Substrate

228 (#102720-100, Agilent Seahorse Bioscience). Briefly, primary tubule cells were isolated from WT
229 and *Acss2^{-/-}* mice and were cultured in a Seahorse 96-well plate at a density of 5×10^3 cells per
230 well. The day before performing the OCR analysis, the cell culture medium was replaced with
231 substrate-limited medium (DMEM (#A14430-01), 0.5 mM glucose, 1 mM Glutamax, 0.5 mM
232 carnitine, and 1% FBS) and maintained up to 18 hours. An hour before performing the OCR
233 analysis, the substrate-limited medium was exchanged with FAO assay medium (1x potassium
234 bicarbonate buffer with 2.5 mM glucose, 0.5 mM carnitine, and 5 mM HEPES). Etomoxir (40 μ M)
235 was added 15 minutes before the start of the OCR analysis to the specified wells. Control cells
236 were supplemented with BSA (0.17 mM) while test cells were supplemented with 1 mM palmitic
237 acid conjugated BSA (0.17 mM). The OCR analysis was performed by treating cells with 2 μ M
238 oligomycin, 1 μ M fluoro-carbonyl cyanide phenylhydrazone (FCCP), and 0.5 μ M rotenone plus 1
239 μ M antimycin A at final concentration.

240

241 **In vivo DNL tracing with deuterated water**

242 DNL tracing was performed at the GC-MS core at the University of Pennsylvania(10). To assess
243 total lipogenesis, mice were subjected to UUO for seven days. On the 6th day, mice were fasted
244 overnight at ~7 pm. On the 7th day, the mice were refed for three hours and then injected with
245 400ul of deuterated water (#151882, Sigma) prepared in 0.9% saline via i.p injection and
246 continued feeding for three more hours. Systemic blood was collected by cardiac puncture, and
247 livers and kidneys were harvested using clamps pre-cooled in liquid nitrogen. The blood was
248 allowed to coagulate on ice for 15 min, and spun down at 10,000g for 5 min at 4C to collect serum.
249 The frozen liver and kidney samples were ground at liquid nitrogen temperature with a Cryomill
250 (Qiagen). Saponification of lipids and gas chromatography–mass spectrometry (GC–MS) analysis
251 were performed at the GC-MS core. Briefly, 5 μ l of serum, and 100 mg of liver or kidney powder
252 was saponified, and fatty acids were extracted by adding 0.5 ml of hexane, vortexing, and

253 transferring the top hexane layer to a new glass vial. Separation was performed by reversed-
254 phase ion-pairing chromatography on a C8 column coupled to negative-ion mode, full-scan GC-
255 MS at 1-Hz scan time and 100,000 resolving power (Agilent 7890A Gas Chromatograph; 5975
256 Mass Spectrometer; Thermo Fischer Scientific). Palmitate was analyzed using GC-MS, and the
257 absolute amount of newly made palmitate was assumed equivalent to the rate of DNL. Data
258 analysis with MAVEN software and natural isotope correction were performed by the GC-MS core.

259

260 **Kidney Triglycerides quantification**

261 Kidney triglycerides were measured using Triglyceride Calorimetric Assay kit (#10010303,
262 Cayman). Approximately 20mg of kidney tissue was homogenized in NP40-substitute assay
263 buffer containing protease and phosphatase inhibitors. Homogenates were collected after
264 centrifuging at 10,000g for 10min at 4°C.

265

266 **Oil Red O staining**

267 For Oil Red O staining, we cut 5µm thin frozen sections. Briefly, the sections were dried at RT for
268 15min and fixed in prechilled 10% formalin buffered PBS for 10min. Slides were washed three
269 times with water for 5min, and finally rinsed in 60% isopropanol for 5min. Lipids were stained by
270 incubating slides in fresh Oil Red 'O' working solution for 30-60min at RT and rinsed in 60%
271 isopropanol for five seconds. Slides were washed three times with water and counterstained with
272 hematoxylin for 3min. Finally, slides were washed in 70% ethanol and mounted with 90% glycerol,
273 and immediately proceeded for microscopic analysis. Images were acquired in EVOS FL inverted
274 fluorescence microscope (#12-563-460, Invitrogen).

275

276 **NADPH/NADP+ ratio measurements**

277 The NADPH/NADP+ ratio was calculated according to the manufacturer protocol (#G1009,
278 Promega). Briefly, an equal number of cells were cultured in a 96-well format and starved
279 overnight for TGF- β 1 treatments. Next, the cells were lysed in 20% DTAB containing Basic
280 solution for 10min at RT. Samples were processed according to the protocol for measuring
281 NADPH and NADP+ from the same well simultaneously. The absolute and relative
282 NADPH/NADP+ values were calculated according to the manufacturer's formula.

283

284 **GSH/GSSH ratio**

285 Reduced and oxidized glutathione levels were measured according to the Glutathione
286 Colorimetric Detection Kit (#EIAGSHC, Thermo Scientific) from the same well after completion of
287 all treatments.

288

289 **Mitochondrial Quality assessments and Mitophagy**

290 Primary cells were cultured on microscopic cover glass overnight until they reached 70%
291 confluency. Cells were incubated in a 5 μ M MitoSox (#M36008, Thermo Scientific) solution for
292 10min in incubator and processed for imaging and quantifications. Cells were also incubated in
293 10 μ M JC-1 (#T3168, Thermo Scientific) for 10min and then proceeded with imaging and
294 quantifications.

295 Mitophagy was assessed as described in our earlier paper (11). Primary cells were transfected
296 with Mito 'Q' mCherry-eGFP COX8 plasmid (#78520, Addgene) for 48h. Cells were processed for
297 various treatments and proceeded with imaging.

298 Cells cultured as above and pretreated with 100 μ M MitoTempo (#SML0737, Sigma) for 2h,
299 followed by TGF- β 1 treatments while MitoTempo was still present. The images of JC-1, mitosox
300 stainings, Mito 'Q' mCherry-eGFP COX8, and MitoTempo experiments were all acquired in
301 Olympus 5000 microscope with Cell Sense software.

302

303 ***In situ* hybridization**

304 *In situ* hybridization was performed on formalin-fixed paraffin-embedded tissue sections using the
305 RNAscope 2.5 HD Duplex Detection Kit (#322436, ACD Bio) according to the manufacture
306 protocol. Freshly cut kidney tissue sections were used in all *in situ* experiments. For the Gsdmd
307 *in situ* hybridization, the antigen retrieval was performed for 30min in heated water bath. The
308 following probes were used for the RNAscope *in situ* assay: Mm Acss2, Hs-ACSS2, Mm-Gsdmd,
309 Mm-Lrp2, Hs-LRP2 and Mm-Hnf4a. *In situ* hybridization quantification was performed manually
310 according to the ACD Bio RNAscope 2.5 HD Duplex user manual.

311

312 Human kidney bulk RNA-seq, and single nuclear RNA sequencing data (previously generated)
313 can be viewed at the http://www.susztaklab.com/hk_genemap/scRNA website.

314

315

316 **References**

317

318 1. Qiu C, et al. Renal compartment-specific genetic variation analyses identify new pathways in
319 chronic kidney disease. *Nat Med.* 2018;24(11):1721-1731.

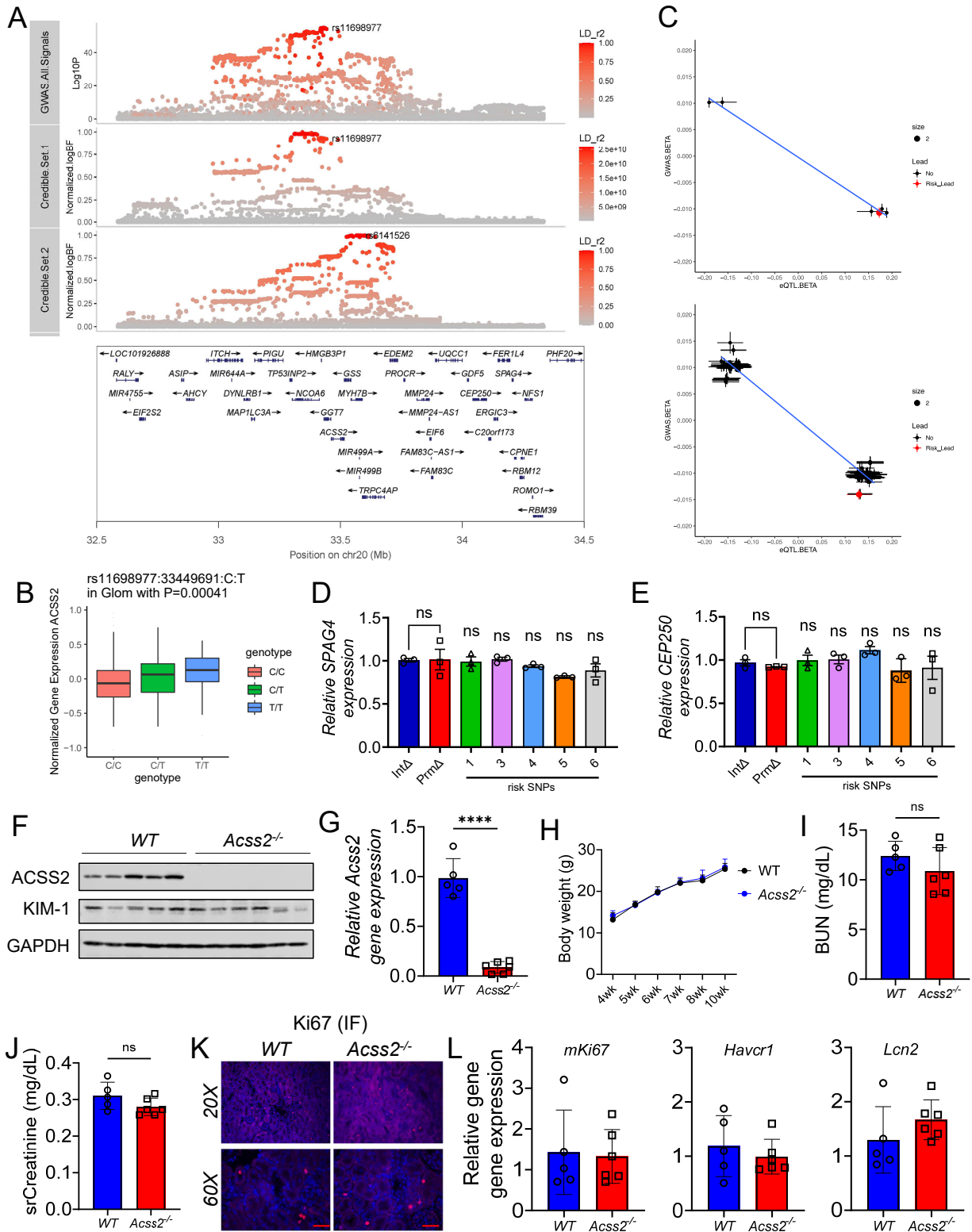
320 2. Sheng X, et al. Mapping the genetic architecture of human traits to cell types in the kidney

321 identifies mechanisms of disease and potential treatments. *Nat Genet.* 2021;53(9):1322-1333.

- 322 3. Liu H, et al. Epigenomic and transcriptomic analyses define core cell types, genes and targetable
323 mechanisms for kidney disease. *Nat Genet.* 2022;54(7):950-962.
- 324 4. Nasser J, et al. Genome-wide enhancer maps link risk variants to disease genes. *Nature.*
325 2021;593(7858):238-243.
- 326 5. Rahman A, et al. A novel approach to adenine-induced chronic kidney disease associated anemia
327 in rodents. *PLoS One.* 2018;13(2):e0192531.
- 328 6. Concordet JP, and Haeussler M. CRISPOR: intuitive guide selection for CRISPR/Cas9 genome
329 editing experiments and screens. *Nucleic Acids Res.* 2018;46(W1):W242-W245.
- 330 7. Mukhi D, et al. Growth hormone induces transforming growth factor-beta1 in podocytes:
331 Implications in podocytopathy and proteinuria. *Biochim Biophys Acta Mol Cell Res.*
332 2023;1870(2):119391.
- 333 8. Zhao S, et al. ATP-Citrate Lyase Controls a Glucose-to-Acetate Metabolic Switch. *Cell Rep.*
334 2016;17(4):1037-1052.
- 335 9. Mukherjee S, et al. SIRT3 is required for liver regeneration but not for the beneficial effect of
336 nicotinamide riboside. *JCI Insight.* 2021;6(7).
- 337 10. Wan M, et al. Postprandial hepatic lipid metabolism requires signaling through Akt2
338 independent of the transcription factors FoxA2, FoxO1, and SREBP1c. *Cell Metab.*
339 2011;14(4):516-527.
- 340 11. Doke T, et al. Genome-wide association studies identify the role of caspase-9 in kidney disease.
341 *Sci Adv.* 2021;7(45):eabi8051.

342

343



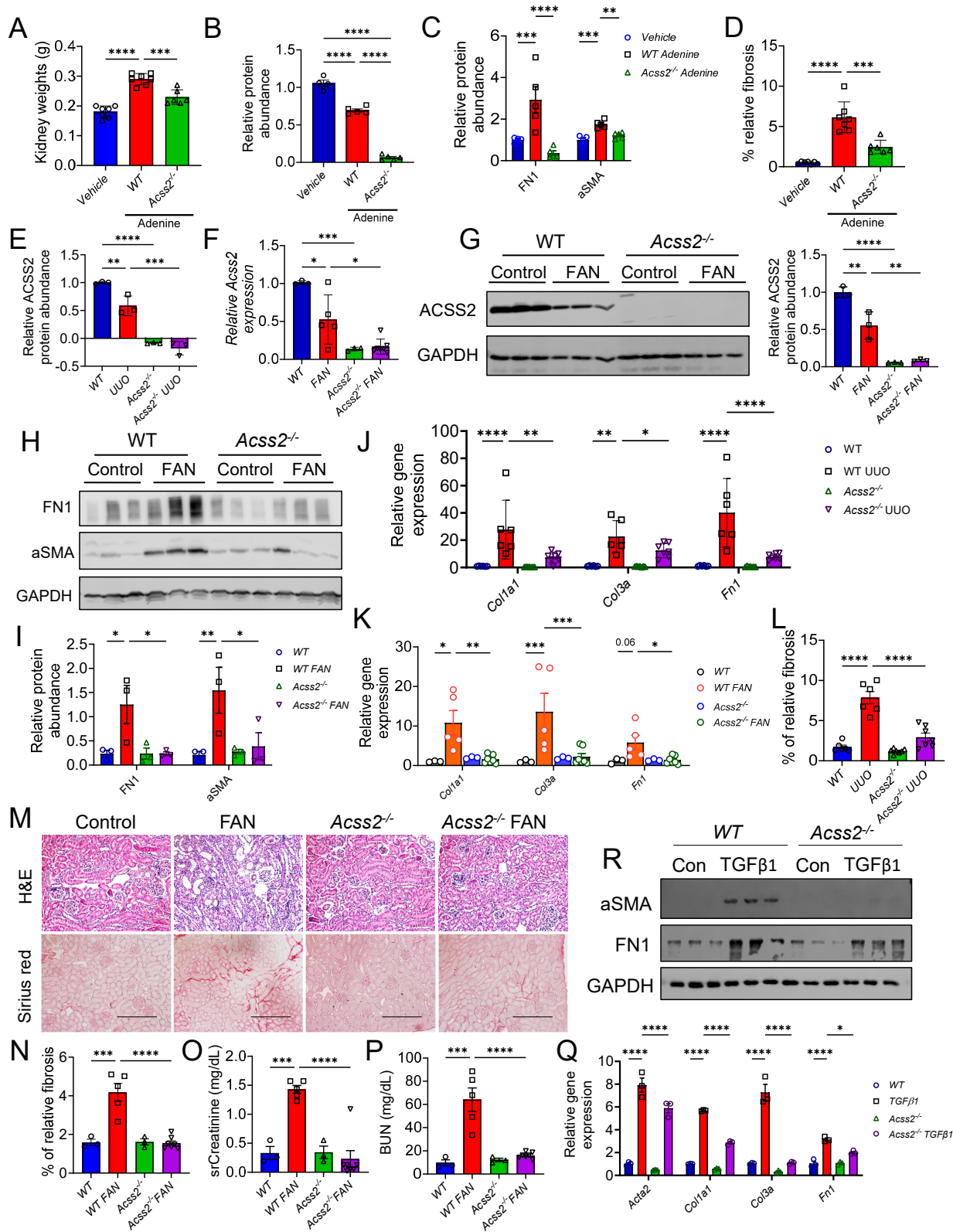
344

345

Supplemental Figure 1. Prioritization of ACSS2 as a kidney disease risk gene.

- 346 A. Fine mapping regional plot showing single nucleotide variants associated with kidney
347 eGFR GWAS dataset (N=1.5M European population). X-axis chromosomal location and
348 y-axis shows the strength of association (-log(p)). Variants shown in red color indicates
349 correlation (extreme right r²) with underlying genes. Color key indicates linkage
350 disequilibrium (r²).
- 351 B. Human kidney *ACSS2* gene expression in glomeruli (n=303) in microdissected samples.
352 Y -axis shows normalized *ACSS2* expression and X-axis shows genotype information.
- 353 C. GWAS and eQTL effect sizes (upper plot tubule; lower plot glom) plotted for *ACSS2* gene
354 in 1.5M human samples.
- 355 D. Transcript levels of *CEP250* following risk regions deleted in HEK293T cells. The data
356 was generated using samples used in Figure 11.
- 357 E. Transcript levels of *SPAG4* following risk regions deleted in HEK293T cells. The data was
358 generated using samples used in Figure 11.
- 359 F. Immunoblots of *ACSS2*, *KIM-1* and *GAPDH* in whole kidney lysates of wild type (*WT*)
360 (n=5) and *Acss2*^{-/-} mice (n=6).
- 361 G. Transcript levels of *Acss2* in kidneys of *WT* (n=5) and *Acss2*^{-/-} mice (n=6).
- 362 H. Weekly body weights recorded in *WT* (n=5) and *Acss2*^{-/-} mice (n=6) at baseline.
- 363 I. Blood urea nitrogen (BUN) in 10 weeks old *WT* (n=5) and *Acss2*^{-/-} (n=6) mice at baseline.
- 364 J. Serum creatinine (sCr) in 10 weeks old *WT* (n=5) and *Acss2*^{-/-} (n=6) mice at baseline.
- 365 K. Ki67 immunofluorescence in *WT* and *Acss2*^{-/-} mice at 10 weeks of age. Scale bars 10μm.
- 366 L. Transcript levels of *mKi67*, *Havcr1* and *Lcn2* in 10 weeks old *WT* (n=5) and *Acss2*^{-/-} (n=6)
367 mice at baseline.

368 Data are represented as mean ± SEM. P values determined by one-way ANOVA for D, E, G, I, J,
369 L after Tukey's multiple comparison. *p < 0.05, **p < 0.01, ***p < 0.001 and ****p < 0.0001. Protein
370 marker was cropped from all blots but was presented in full blots file.



371

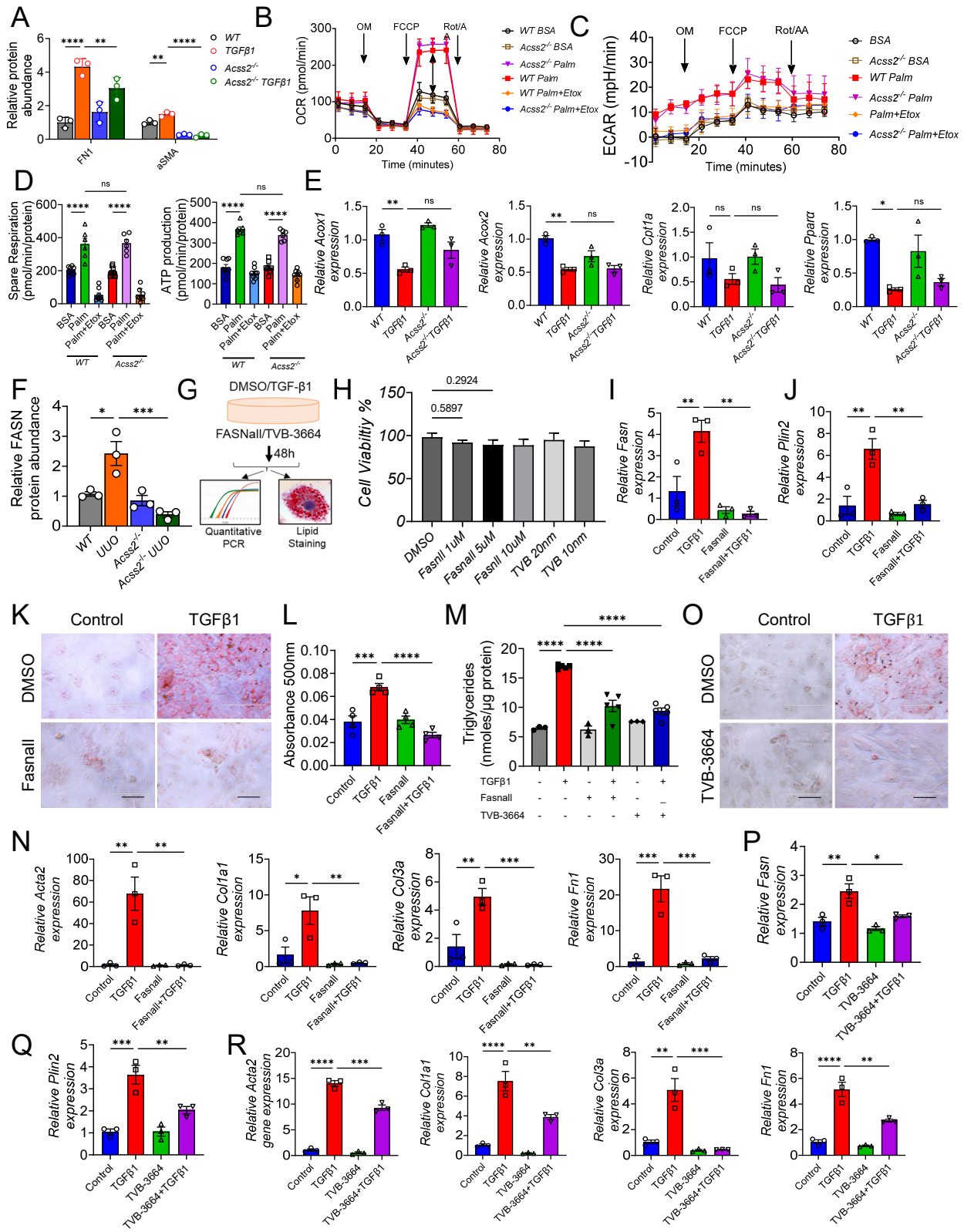
372

Supplemental Figure 2. Loss of ACSS2 protects from kidney disease.

- 373 A. Kidney weights in *WT* (n=7) and *Acss2*^{-/-} (n=6) gavage with adenine.
- 374 B. Quantification of ACSS2 immunoblot in adenine kidneys by image J.
- 375 C. Quantification of FN1, aSMA and GAPDH immunoblots by image J.
- 376 D. Quantification of Sirius red images by image J and plotted as % relative fibrosis area in
377 *WT* (n=7) and *Acss2*^{-/-} (n=6) mice gavage with adenine.
- 378 E. Quantification of ACSS2 immunoblot in unilateral ureteral obstruction (UUO) kidneys by
379 image J.
- 380 F. Transcript levels of *Acss2* in kidneys of *WT* (n=5) and *Acss2*^{-/-} (n=7) mice injected with
381 folic acid (FAN).
- 382 G. (Left) Immunoblot for ACSS2 in FAN kidneys of *WT* and *Acss2*^{-/-} mice. (Right)
383 Quantification of ACSS2 protein levels by image J.
- 384 H. Immunoblots of fibronectin (FN1) and alpha smooth muscle actin (aSMA) in whole kidney
385 lysates of *WT* and *Acss2*^{-/-} mice injected with folic acid.
- 386 I. Quantification of FN1, aSMA and GAPDH immunoblots by image J.
- 387 J. *Collagen 1a1* (*Col1a1*), *collagen type 3a* (*Col3a*) and *fibronectin* (*Fn1*) mRNA levels
388 measured in kidneys of *WT* (n=6) and *Acss2*^{-/-} (n=7) mice in sham and UUO surgery.
- 389 K. *Col1a1*, *Col3a* and *Fn1* mRNA levels in kidneys of *WT* (n=5) and *Acss2*^{-/-} (n=7) mice
390 injected with folic acid.
- 391 L. Quantification of fibrosis by image J in UUO of *WT* (n=6) and *Acss2*^{-/-} (n=7) mice kidneys.
- 392 M. H&E and Sirius red staining images of *WT* and *Acss2*^{-/-} mice injected with folic acid. Scale
393 bars 20µm.
- 394 N. Quantification of Sirius red images by image J and plotted as % relative fibrosis area in
395 *WT* (n=5) and *Acss2*^{-/-} (n=7) mice injected with folic acid.
- 396 O. Creatinine (sCr) levels estimated in serum samples collected from *WT* (n=5) and *Acss2*^{-/-}
397 (n=7) mice injected with folic acid.
- 398 P. Blood urea nitrogen (BUN) levels estimated in serum samples collected from *WT* (n=5)
399 and *Acss2*^{-/-} (n=7) mice injected with folic acid.
- 400 Q. *Acta2*, *Col1a1*, *Col3a* and *Fn1* mRNA levels were measured in tubular epithelial cells
401 (TECs) of *WT* and *Acss2*^{-/-} mice treated with TGFβ1.
- 402 R. Immunoblots for FN1, aSMA and GAPDH in TEC lysates of *WT* and *Acss2*^{-/-} mice.

403 Data are represented as mean ± SEM. P values determined by one-way ANOVA. *p < 0.05, **p
404 < 0.01, ***p < 0.001 and ****p < 0.0001. The data in F-P was a representative data of multiple
405 experiments. Protein marker was cropped from all blots but was presented in full blots file.

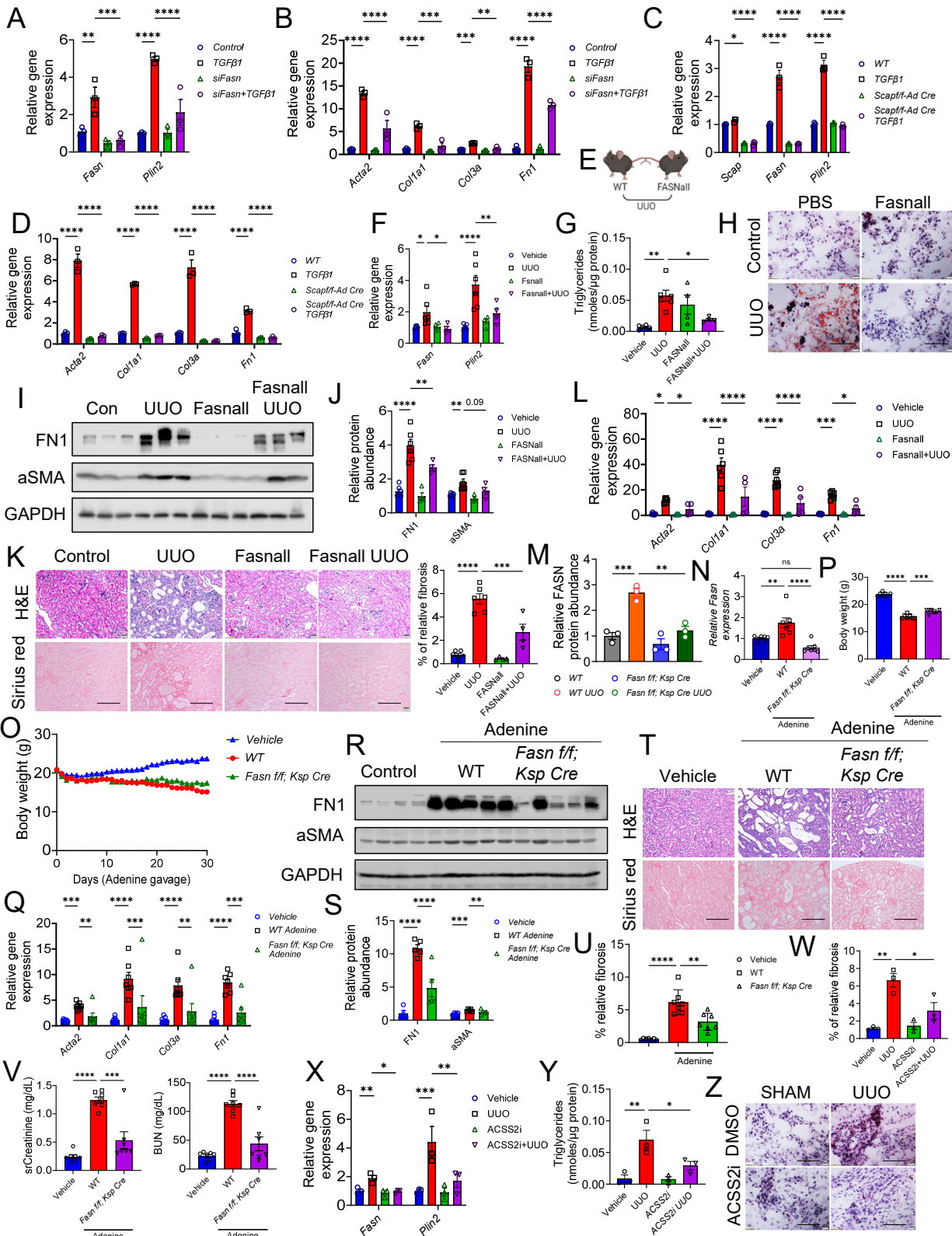
406



Supplemental Figure 3. TGFβ1 induces de novo lipogenesis in primary tubule cells.

- 410 A. Quantification of immunoblots of fibronectin (FN1), alpha smooth muscle actin (aSMA)
411 and GAPDH protein by image J.
- 412 B. Seahorse-based oxygen consumption rate (OCR) in *WT* and *Acss2*^{-/-} primary cells treated
413 with palmitic acid.
- 414 C. Seahorse-based extracellular acidification rate (ECAR) in *WT* and *Acss2*^{-/-} primary cells.
- 415 D. Spare respiration and ATP production by *WT* and *Acss2*^{-/-} cells treated with palmitic acid.
- 416 E. Relative gene expression of *acyl CoA oxidase 1 (Acox1)*, *Acox2*, *carnitine palmitoyl*
417 *transferase 1 (Cpt1a)*, and peroxisome proliferator-activated receptor alpha (*Ppara*) in *WT*
418 and *Acss2*^{-/-} primary tubular epithelial cells (TECs) treated with TGFβ1.
- 419 F. Quantification of fatty acid synthase (FASN) and GAPDH immunoblots in kidneys of *WT*
420 UO and *Acss2*^{-/-} UO by image J.
- 421 G. Experimental scheme.
- 422 H. Cell viability of primary TECs treated with FASNall or TVB-3664.
- 423 I. Relative *Fasn* gene expression in primary TECs treated with TGFβ1 or FASNall.
- 424 J. Relative *perilipin 2 (Plin2)* gene expression in primary TECs treated with TGFβ1 and
425 FASNall.
- 426 K. Oil Red O staining in primary TECs treated with TGFβ1 or FASNall. Scale bars 20μM.
- 427 L. Quantification of Oil Red O staining.
- 428 M. Triglycerides in TECs treated with TGFβ1 and FASNall or TVB-3664.
- 429 N. Relative gene expression of *alpha smooth muscle actin (Acta2)*, *collagen 1a1 (Col1a1)*,
430 *collagen type 3a (Col3a)* and *fibronectin (Fn1)* in primary TECs treated with FASNall or
431 TGFβ1.
- 432 O. Oil Red O staining of primary TECs treated with TGFβ1 or TVB-3664. Scale bars 20μM.
- 433 P. Relative *Fasn* gene expression in primary TECs treated with TGFβ1 or TVB-3664.
- 434 Q. Relative *Plin2* gene expression in primary TECs treated with TGFβ1 or TVB-3664.
- 435 R. Relative gene expression of *Acta2*, *Col1a1*, *Col3a* and *Fn1* in TECs treated with TGFβ1
436 or TVB-3664.

437 All graphs present means of ± SEM. P values determined by one-way ANOVA for panels A, and
438 D-R. *p < 0.05, **p < 0.01, ***p < 0.001 and ****p < 0.0001. The data was a representative of
439 multiple experiments.



440

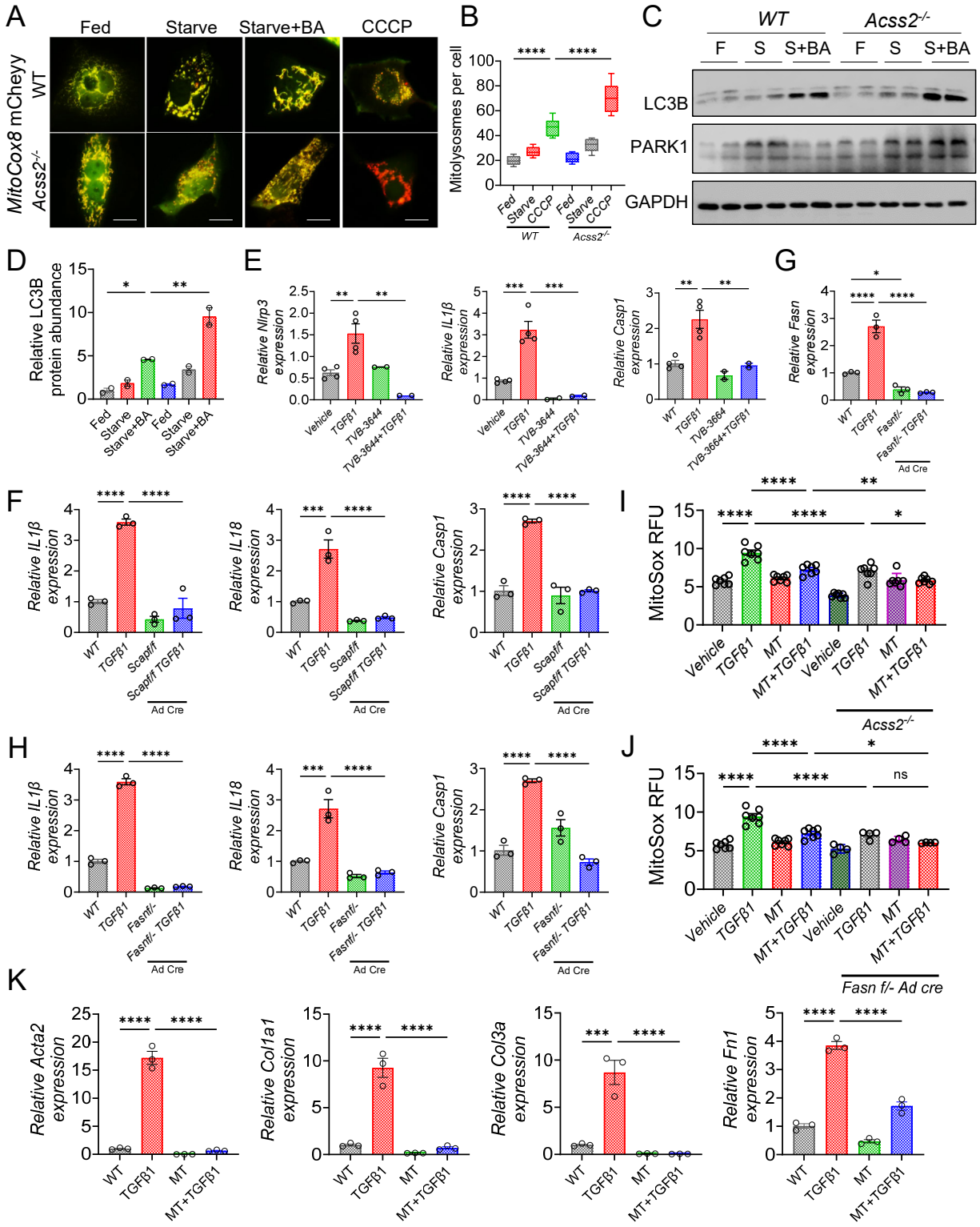
441 Supplemental Figure 4. Inhibition of *de novo* lipogenesis prevents kidney fibrosis.

- 442 A. Gene expression level of fatty acid synthase (*Fasn*) and perilipin 2 (*Plin2*) in TECs
443 transfected with small interfering RNA against *Fasn* (*siFasn*) and treated with TGFβ1 for
444 48h.
- 445 B. Gene expression levels of *alpha smooth muscle actin* (*Acta2*), *Collagen 1a1* (*Col1a1*),
446 *collagen type 3a* (*Col3a*) and *fibronectin* (*Fn1*) in TECs transfected with *siFasn* and treated
447 with TGFβ1.
- 448 C. Gene expression level of *sterol regulatory element binding protein* (*SREBP*) *cleavage*
449 *activating protein* (*Scap*), *Fasn*, and *Plin2* were measured in *WT* and *Scap^{ff}* TECs treated
450 with Adeno-Cre virus (Ad-Cre) for 24h and treated with TGFβ1 for 48h.
- 451 D. Gene expression level of *Acta2*, *Col1a1*, *Col3a* and *Fn1* measured in *WT* and *Scap^{ff}*
452 TECs treated with Ad-Cre and TGFβ1. *WT* and TGF β1 treated samples are the same as
453 used in supplemental figure 2 panel O.
- 454 E. Experimental design.
- 455 F. Gene expression level of *Fasn* and *Plin2* in kidneys of mice injected with FASNall or PBS
456 followed by UUO injury.
- 457 G. Kidney triglyceride levels in mice injected with FASNall or PBS and subjected to UUO
458 injury.
- 459 H. Oil Red O-stained kidney sections of mice injected with FASNall, or PBS followed by UUO
460 injury. Scale bars 10μm.
- 461 I. FN1, aSMA and GAPDH immunoblots in kidneys of mice injected with FASNall or PBS
462 followed by UUO injury.
- 463 J. Quantification of immunoblots of aSMA and FN1 proteins in whole kidney lysates of UUO
464 and FASNall treated UUO mice in image J.
- 465 K. (Left) H&E and Sirius Red staining in kidney sections of mice injected with FASNall or
466 PBS in followed by UUO injury. Scale bars 20μm. (Right) Percentage of fibrosis quantified
467 in image J.
- 468 L. Gene expression level of *Acta2*, *Col1a1*, *Col3a* and *Fn1* in kidneys of mice injected with
469 FASNall or PBS in followed by UUO injury.
- 470 M. Quantification of FASN and GAPDH immunoblots of *Fasn f/f; Ksp Cre* mice with or without
471 UUO.
- 472 N. *Fasn* gene expression levels in *Fasn f/f; Ksp Cre* (n=7) and *WT* (n=7) mice treated with
473 adenine.
- 474 O. Daily body weights in adenine-CKD model of *Fasn f/f; Ksp Cre* (n=7) and *WT* (n=7) mice.
- 475 P. Final body weights of *Fasn f/f; Ksp Cre* (n=7) and *WT* (n=7) mice treated with adenine.

- 476 Q. Gene expression level of *Acta2*, *Col1a1*, *Col3a* and *Fn1* in *WT* (n=7) and *Fasn f/f; Ksp*
477 *Cre* (n=7) mice gavage with adenine.
- 478 R. FN1, aSMA and GAPDH immunoblots in kidneys of mice gavage with adenine in *WT* (n=5)
479 and *Fasn f/f; Ksp Cre* (n=5).
- 480 S. Quantification of FN1, aSMA and GAPDH immunoblots of *Fasn f/f; Ksp Cre* and *WT* mice
481 gavage with adenine.
- 482 T. H&E and Sirius Red staining in kidney sections of mice treated with adenine or vehicle.
483 Scale bars 20µm.
- 484 U. Quantification of Sirius red staining in image J in kidneys of mice gavaged with adenine in
485 *WT* and *Fasn f/f; Ksp Cre* mice.
- 486 V. Serum creatinine (sCr) and blood urea nitrogen (BUN) estimated in *WT* (n=7) and *Fasn*
487 *f/f; Ksp Cre* (n=7) mice gavage with adenine.
- 488 W. Quantification of Sirius red staining in kidneys mice with UUO or ACSS2i treatment.
- 489 X. Gene expression levels of *Fasn* and *Plin2* in *WT* (n=3) and ACSS2i (n=3) injected control
490 and UUO kidneys.
- 491 Y. Kidney triglycerides n kidneys of *WT* (n=3) and ACSS2i (n=3) injected control and UUO
492 kidneys.
- 493 Z. Oil Red O staining in fresh kidney sections of *WT* and ACSS2i injected control and UUO
494 mice. Scale bars 10µm.

495 Data are represented as mean ± SEM. P values determined by one-way ANOVA after Tukey's
496 multiple comparison. *p < 0.05, **p < 0.01, ***p < 0.001 and ****p < 0.0001. WT and TGFβ1 data
497 in panel D was the same as used in data panel Q of supplementary figure 2. Controls and WT
498 adenine samples in panels N-V are the same for *Acss2^{-/-}* and *Fasn f/f; Ksp Cre* adenine
499 experiments. Protein marker was cropped from all blots but was presented in full blots file.

500



501

502 **Supplemental Figure 5. Suppression of mitochondrial ROS suppresses NLRP3-**
 503 **inflammasome activation in primary tubular cells.**

504 A. Mitophagy was assessed in primary tubular epithelial cells (TECs) transfected with
505 mitoCox8 eGFP-mCherry plasmid and subjected to various mitophagy inducers for 2h.
506 Scale bars 10 μ m.

507 B. Mitolysosomes quantified in Image J.

508 C. Immunoblots of LC3B and Parkin1 in primary TECs in fed, starve, and bafilomycin (BA).

509 D. Quantification of immunoblots of LC3B in Image J.

510 E. Relative gene expression of *Nlrp3*, *IL1B*, and caspase1 (*Casp1*) in TECs treated with TVB-
511 3664 or TGF β 1 for 48hr.

512 F. Relative gene expression of *IL1B*, *IL18* and *Casp1* in *WT* and *Scap1*^{-/-} TECs transfected
513 with Adeno-Cre virus (Ad-Cre) and treated with TGF β 1.

514 G. Relative gene expression of *Fasn* in *WT* and *Fasn*^{-/-} TECs transfected with Ad-Cre and
515 treated with TGF β 1. *WT* and TGF β 1 samples are same used in the supplementary figure
516 4 panel C.

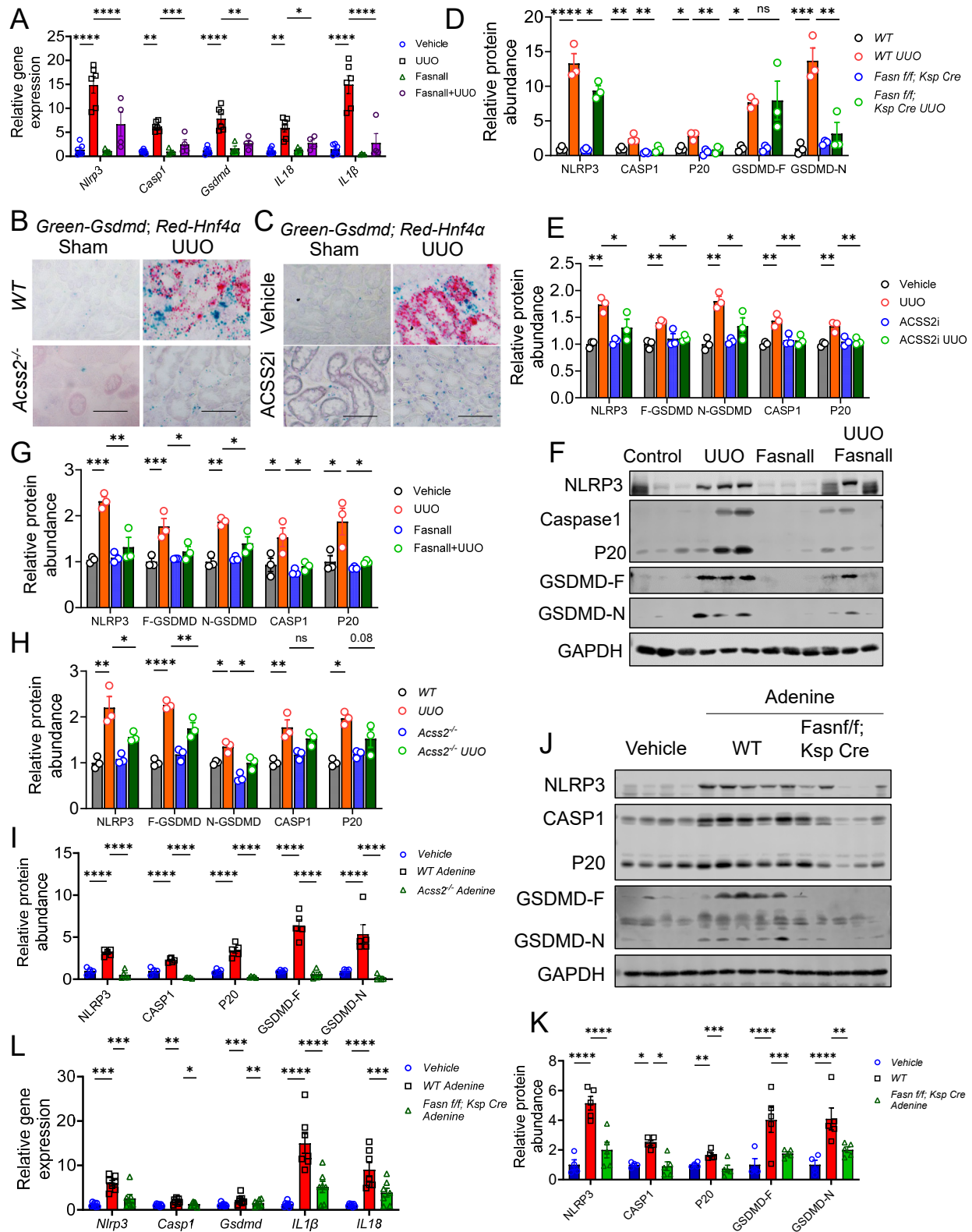
517 H. Relative gene expression of *IL1B*, *IL18* and *Casp1* *WT* and *Fasn*^{-/-} TECs transfected with
518 Ad-Cre and treated with TGF β 1.

519 I. Relative fluorescence of MitoSox quantified in *WT* and *Acss2*^{-/-} cells treated with vehicle
520 or TGF β 1 or mitoTempo (MT).

521 J. Relative fluorescence of MitoSox quantified in *WT* and *Fasn*^{-/-} cells transfected with Ad
522 Cre for 24h and treated with vehicle or TGF β 1 or MT.

523 K. Relative gene expression of *alpha smooth muscle actin (Acta2)*, *Collagen 1a1 (Col1a1)*,
524 *collagen type 3a (Col3a)* and *fibronectin (Fn1)* measured in primary TECs treated with
525 TGF β 1 or MT.

526 Data are represented as mean \pm SEM. P values determined by one-way ANOVA after Tukey's
527 multiple comparison. *p < 0.05, **p < 0.01, ***p < 0.001 and ****p < 0.0001. Vehicle, TGF β 1, MT,
528 and MT+TGF β 1 data are the same for both panels I and J. The data was a representative of
529 multiple experiments. Protein marker was cropped from all blots but was presented in full blots
530 file.

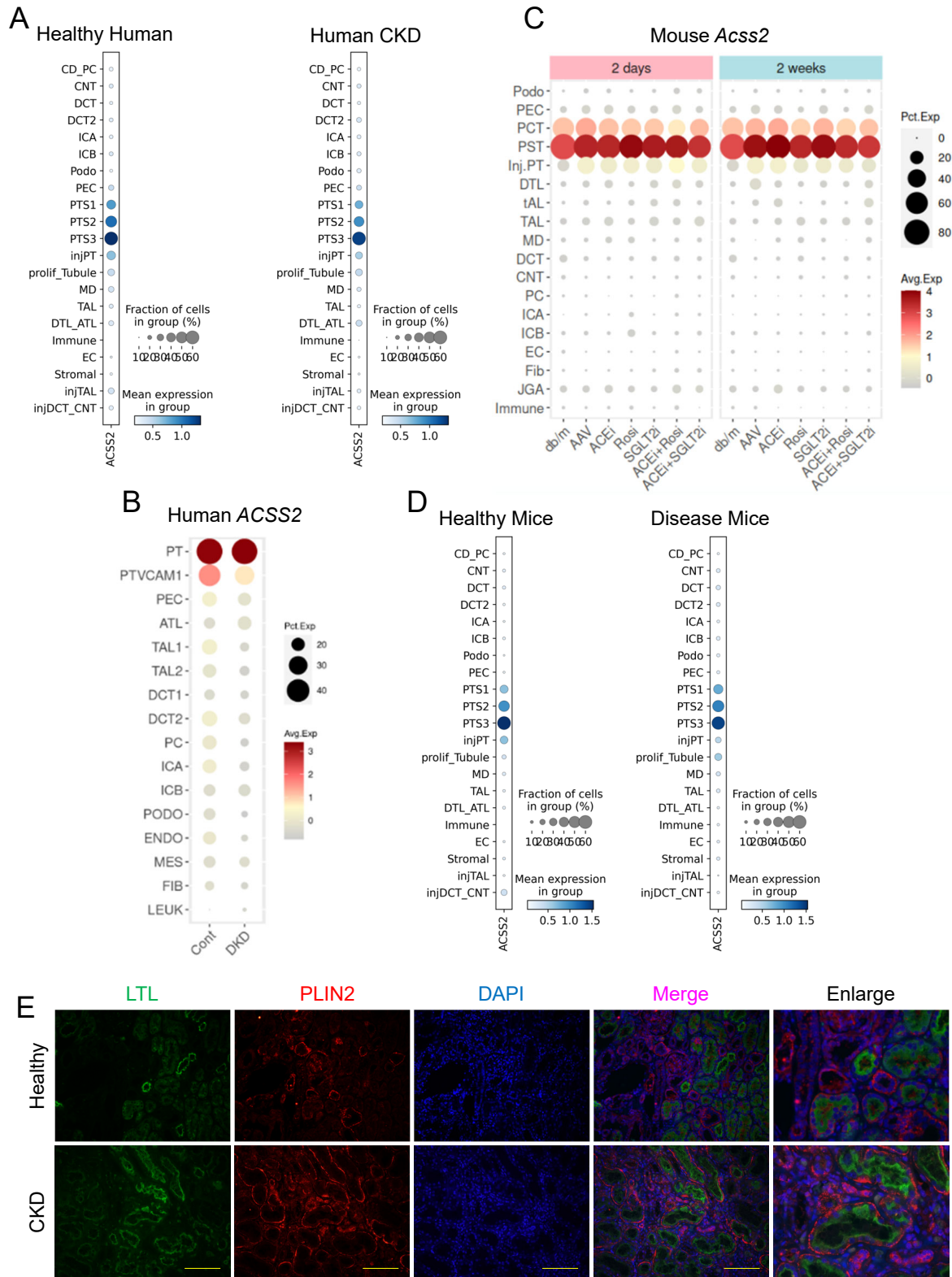


531

532 **Supplemental Figure 6. Inhibition of de novo lipogenesis suppresses ROS-induced NLRP3**
 533 **inflammasome activation.**

- 534 A. Gene expression levels of *Nlrp3*, caspase1 (*Casp1*), *Gasdermin D* (*Gsdmd*), *IL1B*, and
535 *IL18* measured in kidneys of mice injected with vehicle (n=6) or FASNall (n=4).
- 536 B. In situ hybridization of mouse *Gsdmd* in kidneys of *WT* and *Acss2^{-/-}* mice with unilateral
537 ureteral obstruction (UUO) (upper panel) and its quantification (lower panel). HNF-4A was
538 used to detect proximal tubule (PT) cells. Scale bars 10µm.
- 539 C. In situ hybridization of mouse *Gsdmd* in kidneys of mice injected with ACSS2i or UUO
540 injury (upper panel) and its quantification (lower panel). HNF-4A was used to detect
541 proximal tubule (PT) cells. Scale bars 10µm.
- 542 D. Quantification of immunoblots of NLRP3, CASP1, P20 (Cleaved-CASPASE1), GSDMD-F
543 (GSDMD-Full length), GSDMD-N (cleaved-GSDMD) and GAPDH in control and UUO
544 kidneys of *WT* and *Fasn f/f; Ksp Cre* mice.
- 545 E. Quantification of immunoblots performed for NLRP3, total and p20 forms of Caspase1 and
546 full length GSDMD and N-GSDMD in *WT* UUO and ACSS2i injected UUO mice.
- 547 F. Immunoblots of NLRP3, CASP1, P20, GSDMD-F, GSDMD-N and GAPDH in kidney
548 lysates of mice injected with vehicle (n=6) or FASNall (n=4).
- 549 G. Quantification of immunoblots of NLRP3, CASP1, P20, GSDMD-F, GSDMD-N and
550 GAPDH in vehicle or FASNall injected mice with UUO.
- 551 H. Quantification of immunoblots performed for NLRP3, total and P20 forms of CASP1 and
552 GSDMD-F and GSDMD-N in *WT* UUO and *Acss2^{-/-}* mice subjected to UUO.
- 553 I. Quantification of immunoblots of NLRP3, CASP1, P20, GSDMD-F, GSDMD-N and
554 GAPDH in vehicle (n=4), *WT* (n=5) and *Acss2^{-/-}* (n=5) mice gavaged with adenine.
- 555 J. Immunoblots of NLRP3, CASP1, P20, GSDMD-F, GSDMD-N and GAPDH in vehicle
556 (n=4), *WT* (n=5) and *Fasn f/f; Ksp Cre* (n=5) mice gavaged with adenine.
- 557 K. Quantification of immunoblots of NLRP3, CASP1, P20, GSDMD-F, GSDMD-N and
558 GAPDH in vehicle (n=4), *WT* (n=5) and *Fasn f/f; Ksp Cre* (n=5) mice gavaged with adenine.
- 559 L. Gene expression of levels of *Nlrp3*, *Casp1*, (*Gsdmd*), *IL1β*, and *IL18* measured in kidneys
560 of mice injected with vehicle (n=7), or adenine gavage in *WT* (n=7) and *Fasn f/f; Ksp Cre*
561 (n=7) mice.

562 Data are represented as mean ± SEM. P values determined by one-way ANOVA after Tukey's
563 multiple comparison. *p < 0.05, **p < 0.01, ***p < 0.001 and ****p < 0.0001. Controls and *WT*
564 adenine samples are the same for both *Acss2^{-/-}* and *Fasn f/f; Ksp Cre* adenine experiment. Protein
565 marker was cropped from all blots but was presented in full blots file.



566

567 **Supplemental Figure 7. Fatty acid synthesis correlated with fibrosis in CKD patients.**

- 568 A. ACSS2 gene expression in one million human snRNA-seq atlas from healthy (n=141505
569 cells) and chronic kidney disease patients (n=157897 cells). The size of the bubble
570 correlates with the percent of positive cells, and the color indicates the level of its
571 expression (darker higher). Cell types: collecting duct-principal cells (CD_PC), distal
572 convoluted tubule (DCT 1 and 2), intercalated cells A (IC_A) and intercalated cells B
573 (IC_B), podocytes (Podo), parietal epithelial cells (PEC), proximal tubule (PT), injured PT
574 (injPT), proliferative tubule (prolif_Tubule), macula densa (MD), thick ascending Loop of
575 Henle (TAL), distal thin limb-ascending thin limb (DTL-ATL), immune cells (immune),
576 endothelial cells (Endo), stromal cells (stroma), injured TAL (injTAL), and injured DCT
577 (injDCT_CNT).
- 578 B. ACSS2 gene expression in human snRNA-seq data (n=39,176 cells) from healthy and
579 diabetic kidney disease patients. The size of the bubble correlates with the percent of
580 positive cells, and the color indicates the level of the expression (darker higher). Cell types:
581 VCAM1 positive PT cells (PT-VCAM1+), mesangial (Mes), fibroblasts (Fibro), leukocytes
582 (LEUK).
- 583 C. ACSS2 gene expression in one million mouse kidney single cell RNA-seq (scRNA-seq)
584 atlas. The size of the dot correlates with the percent positive cells, and the color indicates
585 the level of the expression (darker higher). Cell type annotations are the same as in panel
586 B. Juxtaglomerular apparatus (JGA), and immune cells (immune).
- 587 D. ACSS2 gene expression in mouse kidney single cell and snRNA-seq atlas (n=382551
588 control cells, and n=64948 diseased cells). The size of the dot correlates with the percent
589 positive cells, and the color indicates the level of the expression (darker higher). Cell type
590 annotations are the same as in panel A.
- 591 E. Immunofluorescence of PLIN2 in healthy (upper panel) and CKD (lower panel) kidneys of
592 human subjects. LTL was used to stain PT segments of the kidney. Scale bars 20 μ m and
593 enlarge scale is 10 μ m.
- 594
595
596
597
598

599 Supplementary Table 1: Gene prioritization table.

600 This table data is related to Figure 1, E, F, and G, comprising all SNPs that are in this genomic
601 region including genetic evidence, SNP position, target genes and genetic tests.

602

603 Supplementary Table 2: Prioritized SNPs.

604 This table data is related to Figure 1G comprises six prioritized SNPs in establishing ACSS2
605 causal risk for this locus.

606

607 Supplementary Table 3. Guide RNAs and human primers.

608 This table is related to Figure 1I and Supplementary Figure 1, D and E. Includes information on
609 ACSS2 guide RNAs, genotyping primers, and human qPCR primers for the three genes.

610

611 Supplementary Table 4: Mouse gene primers.

612 Mouse primers were used in this study.

S.No	Gene	Forward primer	Reverse primer
1	<i>Acss2</i>	GCTTCTTTCCCATTCCTTCGGT	CCCGGACTCATT CAGGATTG
2	<i>Col1a1</i>	TGCCTGGACCTCCTGGCGAGCGT	AGCAGGTCCGGGAGCACCACGTT
3	<i>Col3a</i>	ACAGCTGGTGAACCTGGAAG	ACCAGGAGATCCATCTCGAC
4	<i>Fn1</i>	ACAAGGTTCCGGGAAGAGGTT	CCGTGTAAGGGTCAAAGCAT
5	<i>Acta2</i>	G TTCAGTGGTGCCTCTGTCA	ACTGGGACGACATGGAAAAG
6	<i>Acox1</i>	CTTGATGGTAGTCCGGAGA	TGGCTTCGAGTGAGGAAGTT
7	<i>Acox2</i>	TACCAACGCCTGTTTGAGTG	TTCCAGCTTTGCATCAGTG
8	<i>Ppara</i>	CGAGAAGGAGAAGCTGTTGG	TCAGCGGGAAGGACTTTATG
9	<i>Hmgcr</i>	CGTAAGCGCAGTTCCTTCC	TTGTAGCCTCACAGTCCTTGG
10	<i>Hmgcs1</i>	GGTCTGATCCCCTTTGGTG	TGTGAAGGACAGAGA AACTGTGG
11	<i>Fdps</i>	TCTTTCTACCTGCCTATTGCG	CTCCAAAGAGATCAAGGTAGTCG

12	<i>Scap</i>	AAGATTTCTGTGCCAGGGAG	CTGTGAAGGGTACTCGCC
13	<i>Srebp1</i>	GGCATGAAACCCGAAGTGGT	AGAGGGAGTGAGAATGCCCC
14	<i>Fasn</i>	GCCAACTCGAGGGACACATC	GGGCTTCACGACTCCATCAC
15	<i>Acaca</i>	GCCTGAGACTGGATCAGTGG	TGTGTGACTGGGCTGTGTGA
16	<i>Plin2</i>	GGATAAGCTCTATGTCTCGTGG	GTCTGGCATGTAGTCTGGAG
17	<i>Cpt1a</i>	GGTCTTCTCGGGTCGAAAGC	TCCTCCCACCAGTCACTCAC
18	<i>Nlrp3</i>	ATTACCCGCCCGAGAAAGG	TCGCAGCAAAGATCCACACAG
19	<i>Il-1β</i>	GCAACTGTTCTGAACTCAACT	ATCTTTTGGGGTCCGTCAACT
20	<i>Il18</i>	ACTGTACAACCGCAGTAATAC	AGTGAACATTACAGATTTATCCC
21	<i>Caspase1</i>	ACAAGGCACGGGACCTATG	TCCCAGTCAGTCCTGGAAATG
22	<i>Gasdermin D</i>	CCATCGGCCTTTGAGAAAGTG	ACACATGAATAACGGGGTTTCC
23	<i>Gapdh</i>	AGGTCGGTGTGAACGGATTTG	TGTAGACCATGTAGTTGAGGTCA

613

614